J. of the Environmental Sciences
Vol. 13, No. 11, 965~985, 2004

Tropical Night (Nocturnal Thermal High) in the Mountainous Coastal City

Hyo Choi

Dept. of Atmospheric Environmental Sciences, Kangnung National University, Gangneung 210-702, Korea

(Manuscript received 16 September, 2004 ; accepted 22 November, 2004)

The investigation of driving mechanism for the formation of tropical night in the coastal region, defined as persistent high air temperature over than 25℃ at night was carried out from August 14 through 15, 1995. Convective boundary layer (CBL) of a 1 km depth with big turbulent vertical diffusion coefficients is developed over the ground surface of the inland basin in the west of the mountain and near the top of the mountain, while a depth of thermal internal boundary layer (TIBL) like CBL shrunken by relatively cool sea breeze starting at 100 km off the eastern sea is less than 150 m from the coast along the eastern slope of the mountain. The TIBL extends up to the height of 1500 m parallel to upslope wind combined with valley wind and easterly sea breeze from the sea. As sensible heat flux convergences between the surface and lower atmosphere both at the top of mountain and the inland coast are much greater than on the coastal sea, sensible heat flux should be accumulated inside both the TIBL and the CBL near the mountain top and then, accumulated sensible heat flux under the influence of sea breeze circulation combined with easterly sea breeze from sea to inland and uplifted valley wind from inland to the mountain top returning down toward the eastern coastal sea surface should be transported into the coast, resulting in high air temperatures near the coastal inland. Under nighttime cooling of ground surface after sunset, mountain wind causes the daytime existed westerly wind to be an intensified westerly downslope wind and land breeze further induces it to be strong offshore wind. No sensible heat flux divergence or very small flux divergence occurs in the coast, but the flux divergences are much greater on the top of the mountain and along its eastern slope than on the coastal inland and sea surfaces. Thus, less cooling down of the coastal surface than the mountain surface and sensible heat transfer from warm pool over the coast into the coastal surface produce nocturnal high air temperature on the coastal inland surfaces, which is not much changed from daytime ones, resulting in the persistence of tropical night (nocturnal thermal high) until the early in the morning.

Key Words : Tropical night, Nocturnal thermal high, Convective boundary layer, Thermal internal boundary layer, Sensible heat flux, Valley wind, Sea breeze, Mountain wind, Land breeze, Warm pool

1. Introduction

Tropical night (Nocturnal thermal high), which is persistent hot night with air temperature over than 25 ℃ until the early morning is one of interesting topics in the northern Asian countries in recent ten years. During the past decade, empirical and numerical studies on wind and heat budget over coastal complex terrain have been carried out for precise prediction, but their inaccurate predictions are due to complicate driving mechanisms of heat and moisture budgets. Raynor et al.[1] explained direct association of heat process in the coastal region with wind and temperature generated by sea-land breeze and Pielke[2] stated both orographic effects with high mountains and the roll of sea breeze on atmospheric circulations near the coast, under the horizontal temperature contrast of air over land and sea surfaces.

Corresponding Author : Hyo Choi, Dept. of Atmospheric Environmental Sciences, Kangnung National University, Gangneung 210-702, Korea
Phone : 033-652-0356
E-mail : du8392@hanmail.net

Kondo et al.[3] emphasized that more sensible heat had to be accumulated in the valley region than over the mountainous areas on calm and cloudless days, due to much larger amplitudes of the diurnal variations of atmospheric temperature and surface pressure at the bottom of a valley. Whiteman[4] explained thermally developed wind system in mountainous terrain through observation and Kuwagata, et al.[5] discussed the daytime boundary layer heating process over complex terrain under fair weather, but they are confined to explain the accumulation of heat in the inland basin, not consider thermal accumulation in the mountainous coastal region. Choi and Kim[6] and Choi[7,8] also verified the formation of nocturnal thermal high in inland basin near Taegu city, in the central part of south Korea by numerical simulation, but no explanation for its formation in the coastal region.

This study is focused on the evolution of nocturnal thermal high (tropical night) in the mountainous coastal basin, instead of inland basin, using a three-dimensional numerical model

2. Numerical analysis and data

The study area has a special topographical feature, which consists of inland plain, high steep mountain, narrow inland basin and sea. In a coarse-mesh domain, Tae Baek mountains lie from south toward north along the eastern coast of Korea and another several branch mountains stretch out toward south-west off the mountains. In a fine-mesh domain, the study area consists of complex terrains characterized by forest in a high steep mountain (Mt. Taegullyung; 865 m above mean sea level) in the west, Kangnung city in the narrow plain of the center and sea in the east (Fig. 1).

A non-hydrostatic grid point model in a complex terrain-following coordinate (x, y, z*) was adopted for a 48 hour numerical experiment from 0600 LST (Local Standard Time = 9h + UTC), August 13 to 0600 LST, August 15, 1995, by HITACHI super computer at Meteorological Research Institute (MRI), Japan Meteorological Agency (JMA). Two different domains consist of 50×50 grid points with a uniform horizontal interval as 20 km in a coarse-mesh model and 5 km in a fine-mesh for one-way double nesting, respectively. 16 levels in the vertical coordinate were divided from

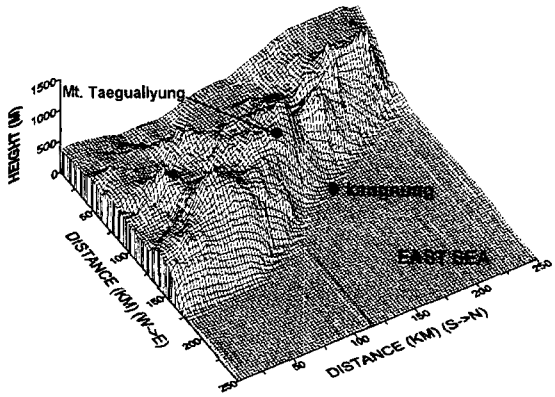

Fig. 1. Topographical feature near Kangnung city.

10m into 6km. 12 hourly global meteorological analysis data made by JMA were horizontally and vertically interpolated for initial data in the coarse domain and predicted ones by the model were treated as lateral boundary data in the fine-mesh. National Oceanic and Atmospheric Administration satellite pictures were used as sea surface temperature in two models.

3. Numerical formula

A three-dimensional non-hydrostatical model in a terrain-following coordinate system called local wind model of JMRI is based upon Boussinesq and anelastic approximations[9,10]. The equations of motion is as follow:

$$d_t hu = f hv - h\theta\,\partial_x \pi + \theta(z_T - z^*)\,\partial_x z_G\,\partial_{z^*}\pi' + z_T^2/h_{z^*}(K_m\,\partial_{z^*}u) \quad (1)$$

$$d_t hv = -f hu - h\theta\,\partial_y \pi + \theta(z_T - z^*)\,\partial_y z_G\,\partial_{z^*}\pi' + z_T^2/h\,\partial_{z^*}(K_m\,\partial_{z^*}v) \quad (2)$$

$$d_t hw = -z_T\theta\,\partial_{z^*}\pi' + gh\theta'/\theta \quad (3)$$

where z* is the terrain-following vertical coordinate defined as

$$z^* = z_T\,(z - z_G)/h$$

$$h = z_T - z_G$$

$$d_t = \partial_t + u\,\partial_x + v\,\partial_y + w^*\,\partial_{z^*}$$

$$hw^* = z_T w + (z^* - z_T)(\partial_x z_G u + \partial_y z_G v)$$

$$\theta = T(1000/P)^{Rd/Cp}$$

$$\theta' = \theta - \bar{\theta}$$

$$\pi = C_p (P/P_{00})^{Rd/Cp}$$

$$\pi = C_p (P/P_{00})$$

$$\pi' = \pi - \bar{\pi}$$

and θ, Θ, T, π, $\bar{\pi}$, π', z, z_T, z_G and K_m imply potential temperature (K), mean potential temperature of the model domain, air temperature at a given height, Exner function of the model atmosphere, Exner function of isentropic atmosphere ($\theta=\Theta$), deviation of π, height of upper boundary with its change for time and place, height of topography and vertical diffusion coefficient for turbulent momentum (m^2/s), respectively. f, g, u, v, w and w^*, P, P_{00}, R_d and C_p are Coriolis parameter, gravity (m/s^2), velocity compoments in the x, y, z and z^* coordinates, atmospheric pressure, pressure at reference level, gas constant for dry air and specific heat at constant pressure.

Radiative heating rate of atmosphere, Q_r and specific humidity, q from thermodynamic equation and conservation of water vapor yields to

$$d_t h\theta' = z_T^2/h\ \partial_{z^*}(K_h\ \partial_{z^*}\theta') + hQ_r \quad (4)$$

$$d_t hq = z_T^2/h\ \partial_{z^*}(K_h\ \partial_{z^*}q) \quad (5)$$

and the continuity equation is

$$\partial_x hu + \partial_y hv + \partial_{z^*} hw^* = 0 \quad (6)$$

Assuming that horizontal scale of the phenomena is one order greater than vertical scale, Eq.(3) for hydrostatic equilibrium case can be converted into the following pressure equations as;

$$\partial_{z^*}\pi' = h/z_T\ g/T^2\theta' \quad (7)$$

In a non-hydrostatic model, hydrostatic pressure deviation, π'_H is given to

$$\partial_{z^*}\pi'_H = h/z_T\ g/T^2\theta' \quad (8)$$

and non-hydrostatic pressure can be calculated as

$$\begin{aligned}\pi'_N &= \pi' - \pi'_H \\ &= r(x, y, z^*)/(\Theta h) \quad (9)\end{aligned}$$

where r is expressed by

$$\begin{aligned}r(x, y, z^*) = {} & \partial_x ADVX + \partial_y ADVY + z_T/h\ \partial_{z^*} ADVZ \\ & + 1/h\ \partial_x z_G\ \partial_{z^*}(z^* - z_T) ADVX \\ & + 1/h\ \partial_y z_G\ \partial_{z^*}(z^* - z_T) ADVY\end{aligned}$$

and

$$\begin{aligned}ADVX = {} & -\partial_x huu - \partial_y huv - \partial_{z^*} huw^* + fhv \\ & -\Theta h\ \partial_x \pi'_N - \Theta(z^* - z_T)\ \partial_x z_G\ \partial_{z^*}\pi'_N \\ & + z_T^2/h\ \partial_{z^*}(K_m\ \partial_{z^*} u)\end{aligned}$$

$$\begin{aligned}ADVY = {} & -\partial_x huv - \partial_y hvv - \partial_{z^*} hvw^* - fhu \\ & -\Theta h\ \partial_y \pi'_N - \Theta(z^* - z_T)\ \partial_y z_G\ \partial_{z^*}\pi'_N \\ & + z_T^2/h\ \partial_{z^*}(K_m\ \partial_{z^*} v)\end{aligned}$$

$$ADVZ = -\partial_x huw - \partial_y hvw - \partial_{z^*} hww^*$$

Time integration of equations and the vertical direction in the z* coordinate were calculated by Euler-backward and Crank-Nicholson schemes. The atmospheric pressure changes at the top of model atmosphere with a material surface were controlled by wave radiation condition suggested by Klemp and Durran[11]. Orlanski[12], periodic lateral boundary condition was applied to the calculation of u, v,$\theta$and q. Time intervals, $\triangle t$=30 s in the coarse-mesh model and $\triangle t$ =10 s in the fine-mesh are determined to effectively reduce external gravity waves in non-hydrostatic model equations.

The vertical diffusion coefficients, K_m and K_h for momentum and heat in the surface boundary layer were evaluated from the turbulent closure level-2 model[13,14]. H_2O and CO_2 transmission functions, effective vapor amount, specific humidity (g/cm^2), pressure (mb) at the surface and arbitrary levels were considered for evaluating total net flux of long wave radiation from the ground surface toward the upper levels. Total net solar radiation at the ground with a function of solar zenith angle, latitude, declination and time angle is calculated by Katayama's[15] scheme for computing radiative transfer in the troposphere.

Newtonian cooling due to long wave radiation and radiative heating rate for air and soil temperatures near the surface were consider in detail. Assuming surface boundary layer to be a constant flux layer for estimating sensible and latent heat fluxes, similarity theory suggested by Businger[16] and Monin[17] is adopted.

A force restore method devised by Deardorff [18] was employed for the time variation of soil temperature and specific humidity at the surface.

4. Results and Discussion

4.1. Synoptic weather condition

On the surface weather map at 0000 UTC, August 14 (0900 Local Standard Time; LST), 1995 in Fig. 2, high pressure of 1016 hPa in the northern China stretches into Manchuria and low pressure of 1008mb is found in the north-eastern part of Korean peninsula near Vladivostok, Russia, while another high of 1022 hPa is in the north-eastern sea of Japan. As the cyclonic motion of low pressure induces dry and hot air masses from Manchuria toward the northern Korea and the high pressure of 1022 hPa also induces moist and hot air masses from the low latitude of the Pacific Ocean near Philippine, cold front generated by two different pressure systems stretches through the central part of Korea into the Yellow Sea. Moderate synoptic-scale south-westerly wind less than 5m/s prevails in the southern part of Korean peninsula. At 0600 UTC (1500 LST), the center of low pressure is still in the same location and wind pattern is not changed (Fig. 2).

On 850 hPa and 700 hPa charts at 0000 UTC, moisture spreads out in the vicinities of cold front, but near Kangnung city, there is no cloud, due to adiabatic heating of air masses compressed by a high pressure of 1022 hPa in the north-eastern East Sea (Fig. 4 and 5). At 1200 UTC (2100 LST), as high pressure of 1016 hPa with a speed of 10 kt approaches into Manchuria and the previous low pressure weaken into 1006 hPa moves to the Sakhalin, the end of cold front also moves to Vladivostok area and cold front disappears in the Korean peninsula.

Thus, high-pressure system of 1016 hPa in the Manchuria strongly influences dry and hot weather condition in the northern part of Korean peninsula, while another high pressure of 1022 hPa in the north-eastern sea of Japan also induces southerly wind with moisture advection into the Korea. However, moist air advected by the southerly wind should be dried out, through adiabatic heating process due to pushing down of air masses by high pressure, resulting in no cloud in the southern part of Korean peninsula, especially Kangnung city in the eastern coastal area of Korea (our study area).

Under clear sky weather condition, strong solar radiation for daytime hours causes thermal heating process of the ground surface to be strong and it could induce the formation of high air temperature in the eastern coastal area and then this high air temperature could persist for nighttime hours. At 2100 LST on 850 hPa chart, cloud band lies on the cold front between high pressure of 1020 hPa in the Manchuria and high pressure of 1022 hPa in the north-eastern sea of Japan and the cloud band affects weather in the only northern part of Korean

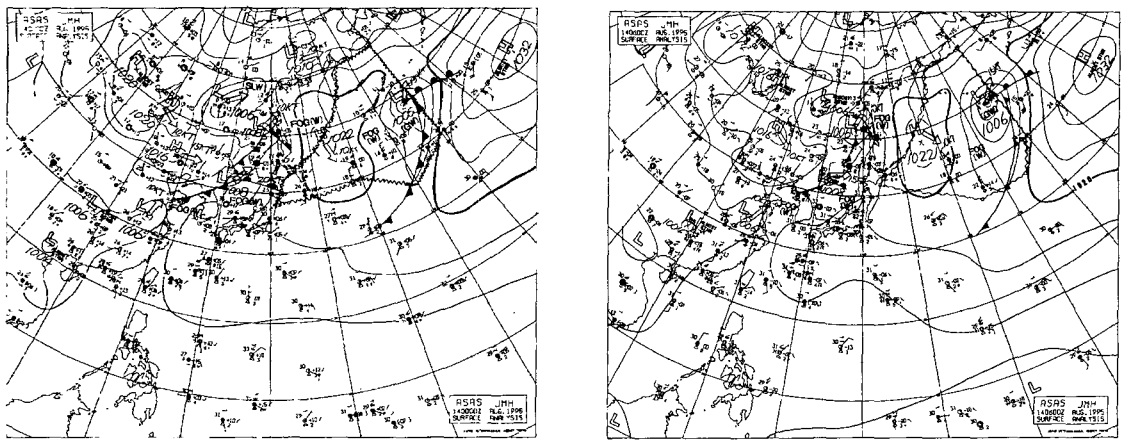

(a) (b)

Fig. 2. Surface weather map (a) at 0000 UTC (0900 LST) and (b) 0600 UTC (1500 LST) on August 14, 1995, supplied by MRI.

peninsula, but no cloud still exists in the Kangnung area. On 700 hPa chart, no cloud is found in the whole Korean peninsula and it continues to be through 1800 UTC (0300 LST, August 15).

At 18z, Korean peninsula is strongly under the influence of high pressure with no cloud shown in Fig. 3 and winds are still in the same patterns. Consequently, from 0000 UTC (0900 LST, August 14) through 1800 UTC (0300 LST, August 15), wind is south-westerly near Kangnung city in the eastern coastal sea of Korea. Among two important reasons on the formation of no cloud near Kangnung city, one is due to synoptic scale adiabatic heating process of air masses under the high pressure and another thing is attributed to local scale adiabatic heating under the compression of air by strong downslope wind along the eastern slope of the high mountain called Taeguallyung in the west of Kangnung city. These adiabatic heating processes of air masses can cause the formation of high air temperature for nighttime hours, resulting in the existence of tropical night over 25℃, until next day morning. Local

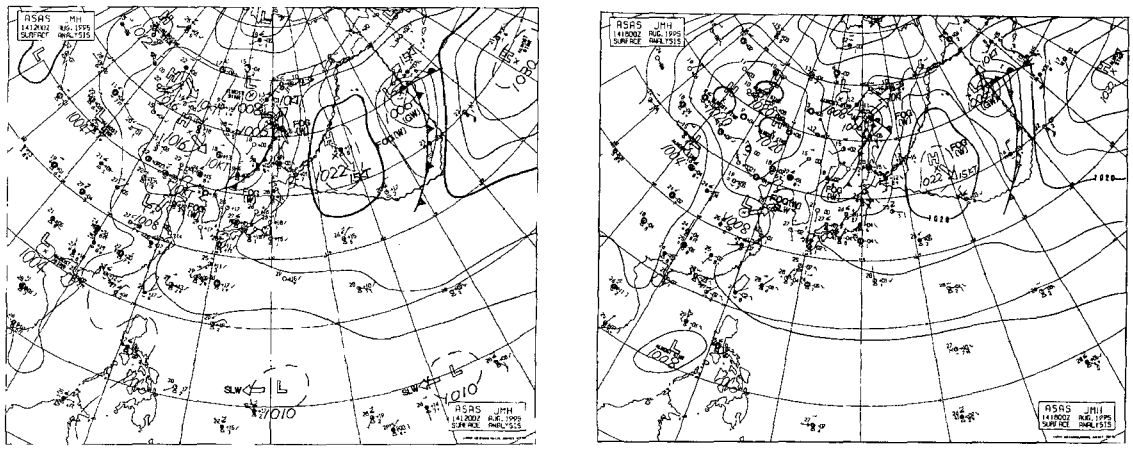

(a) (b)

Fig. 3. As shown in Fig. 2, except for (a) 1200 UTC (2100 LST) and (b) 1800 UTC (0300 LST, August 15) on August 14.

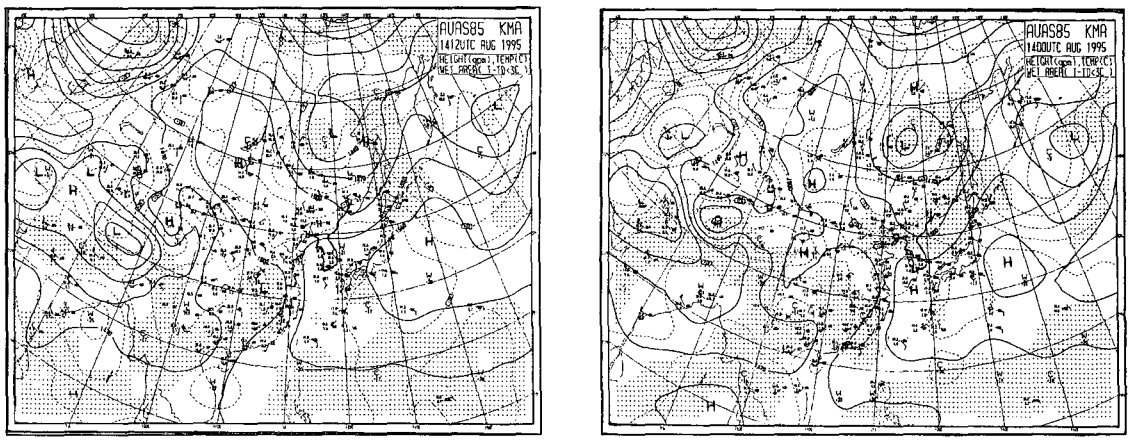

(a) (b)

Fig. 4. 850 hPa chart (a) at 0000 UTC (0900 LST) and (b) 1200 UTC (2100 LST), August 14, 1995, supplied by MRI. Shadow area indicates the region of moisture spreading and no moisture distribution is near Kangnung city in the eastern coast of Korea.

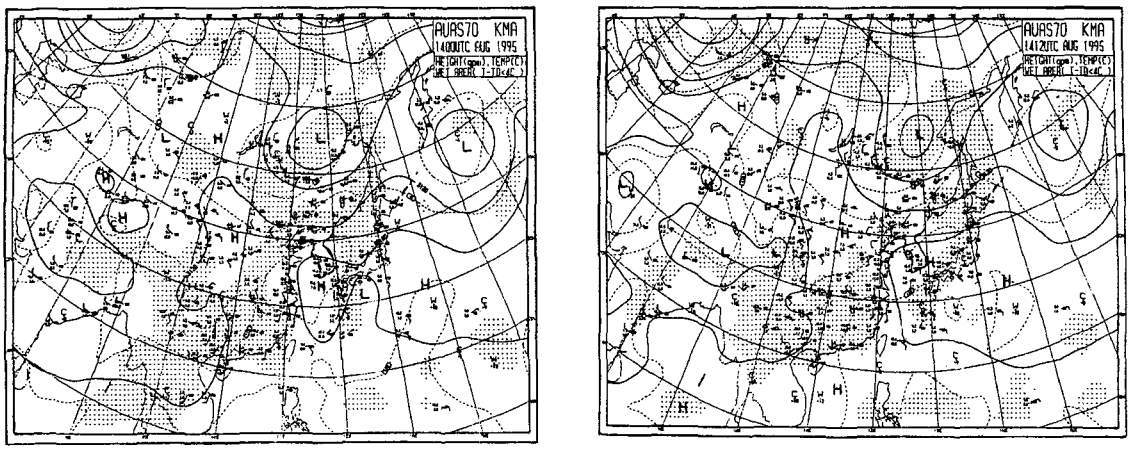

(a) (b)

Fig. 5. 700 hPa chart (a) at 0000 UTC (0900 LST) and (b) 1200 UTC (2100 LST), August 14, 1995, supplied by MRI. Shadow area indicates the region of moisture spreading and no moisture distribution is near Kangnung city in the eastern coast of Korea.

heating process is explained later in detail.

4.2. Wind and heat budget

4.2.1. Wind field-daytime

At 1200LST, August 14, in a coarse-mesh domain, synoptic-scale westerly winds at 10m height over the ground surface prevail over the Yellow Sea and penetrate into the Korean peninsula, passing through eastern coastal mountainous regions near Kangnung city, whose climate under south-westerly wind in the inland shown in Fig. 2 and Fig. 3, but easterly sea breeze is detected in the coastal inland and sea, due to the temperature contrast of air temperature between over land and sea surfaces (Fig. 6a). So, two different wind regimes confront each other in the inland 15 km away from the coast and the intrusion of sea

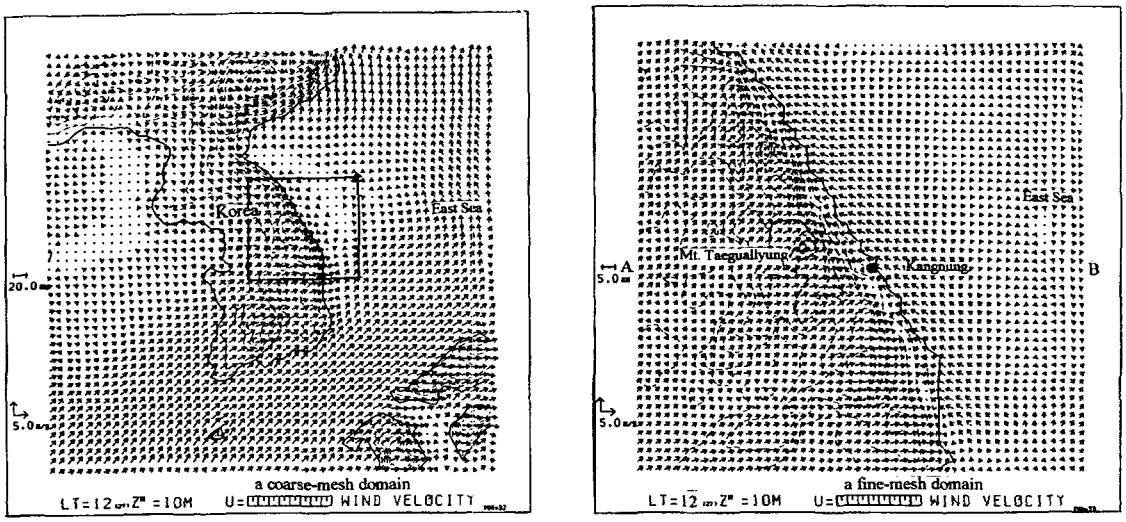

(a) (b)

Fig. 6. (a) Wind (m/s) in a coarse-mesh domain at 1200 LST, August 14, 1995. Thin dash line and box denote topography and fine-mesh domain. (b) Wind (m/s) in a fine-mesh domain near Kangnung city.

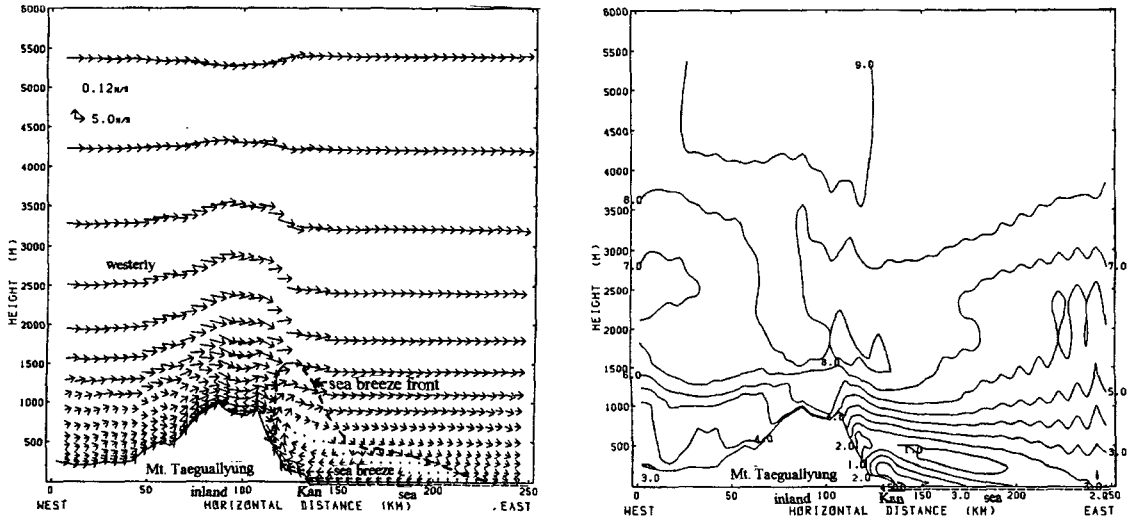

(a) (b)

Fig. 7. (a) Vertical profiles of wind vector (m/s) on a straight cutting line A-B (Mt. Taegeallyung-Kangnung city-East Sea) in a fine-mesh domain as shown in Fig. 6b and (b) wind speed (m/s).

breeze from sea toward inland near is limited to inland 15km near Kangnung city or 20km near Ulchin city in the low latitude.

In Fig. 6b, winds at the city with a high steep Mt. Taegeallyung in the west and the East Sea in the east are still south-westerly. Though wind and temperature in the coarse and fine-mesh domains are similar to observed data, simulations in a fine domain by one-way nesting process produce more accurate values with the same patterns. On vertical profiles of winds in Fig. 7a and 7b, after sea breeze starts at 100 km offshore and combines with valley wind in the coastal plain near Kangnung city, it becomes an intensified upslope wind and reaches the mid of the eastern slope. Simultaneously, prevailing synoptic scale westerly wind blows over Mt. Taegeallyung toward the coast and it confronts the upslope wind along its eastern slope and then, it goes up to the height of 1700 m, finally becoming a return flow in the upper level over the sea. Then, the return flow is separated into two atmospheric circulations, such as a small circulation in the coastal sea and another big one in the open sea.

Namely, since daytime synoptic westerly downslope wind suppresses meso-scale thermally induced easterly upslope flow from the coast toward the mountain top, due to both different heating rate between mountain slope and coastal plain (valley wind) and one between inland coastal plain and sea (sea-breeze), resultant westerly surface wind speed at the mountain top is 4 m/s, but 1.0 m/s at the mid of its slope. Easterly upslope wind speed near the top of the mountain is 5 m/s and 5 m/s at the coastal edge near Kangnung city, but sea breeze in the coastal sea is 3 m/s or 4 m/s.

4.2.2. Turbulent diffusion and heat flux-daytime

In Fig. 8a, turbulent heat in terms of vertical diffusion coefficients for turbulent heat (K_h) can easily present vertical motion of air due to daytime heat process. The values of K_h are more than 120 m^2/s over the plain in the west of the mountain and the top or along the eastern slope of the mountain, but 5 m^2/s over the sea surface. Higher values of the diffusion coefficients are found along the eastern slope than over the sea, due to great diabatic heating on the mountain surface. In the upper atmospheric layer above the height of 1700 m, turbulent heat diffusivity is almost constant and the development of convective boundary layer (CBL) is confined to this level.

So, the CBL is developed with a depth of about 1km over the ground at the upwind side of the mountain, while its depth is only limited to less than 150 m along the eastern slope as thermal internal boundary layer (TIBL) parallel to sea breeze front. The depth of TIBL in the inland coast is 250 m and

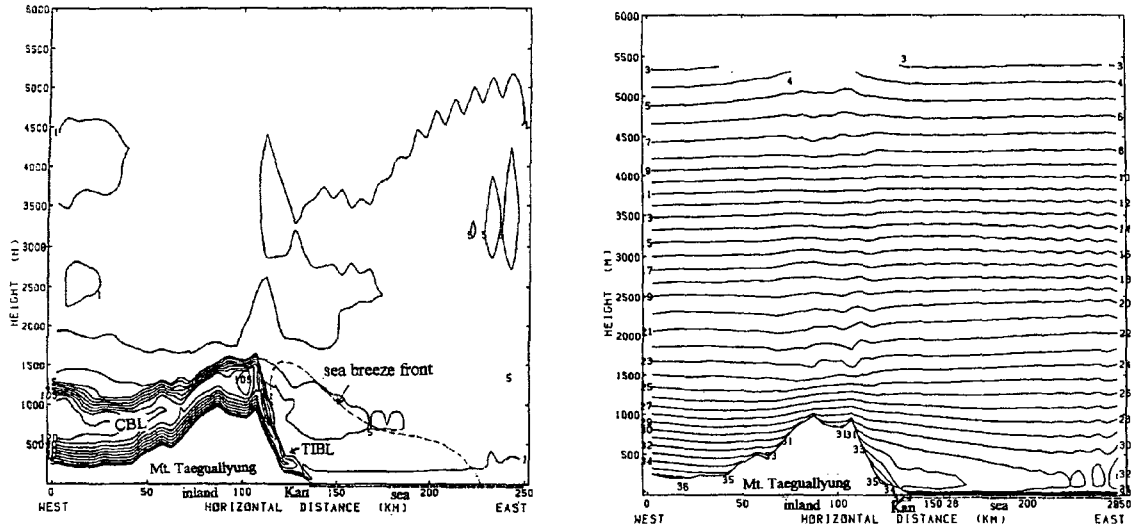

(a) (b)

Fig. 8. (a) As shown in Fig. 7-1 except for vertical diffusion coefficient for turbulent heat (m^2/sec) and (b) air temperature (℃).

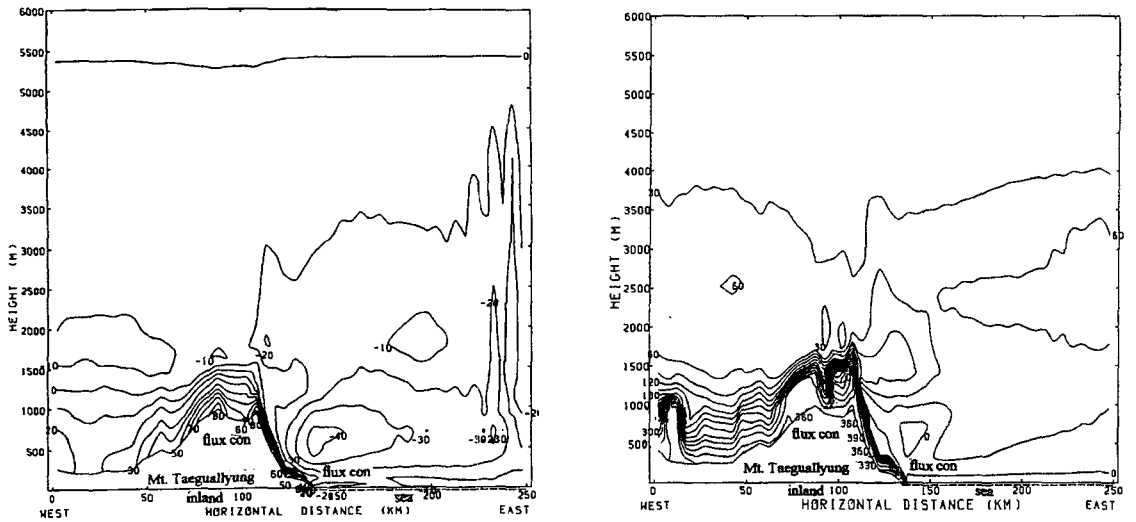

(a) (b)

Fig. 9. (a) As shown in Fig. 7a, except for sensible heat flux (W/m^2) and (b) latent heat flux (W/m^2).

becomes shallow along the slope. Warm and dry air is the inside of TIBL or CBL, while relatively cool and moist air is in the sea breeze front. The formation of shallow TIBL like CBL from the coastal edge along the eastern slope of the mountain is due to the shrunken of CBL cooled down by relatively cool easterly sea breeze and partly due to different surface roughness between land and sea surfaces. In Fig. 8b, maximum air temperature of 35℃ is found near the bottom of the eastern slope, since strong daytime thermal heating at the ground surface on the mountain slope can produce a very high air temperature and westerly downslope wind may make, in part, a contribution to the increase of air temperature due to adiabatic heating processing from compression of air by wind, which exact amount of adiabatic heating

rate has not presently been known in literatures.

In Fig. 9a, sensible heat fluxes from the surface of the top of mountain to the upper level are in a range of 60 W/m^2 to - 20 W/m^2 and those from the inland coast to the upper level are also from 50 W/m^2 to 40 W/m^2, showing flux convergence. On the other hand, the fluxes from the coastal and open sea surfaces to the upper levels are from 20 W/m^2 to 40 W/m^2 and from 10 W/m^2 to 40 W/m^2. As sensible heat fluxes are much greater at both the mountain top and inland coast than in the upper level or slightly greater at the sea surface, flux convergences toward the upper level could cause these surfaces to be warmed up. Since sensible heat flux convergence at the mountain top is stronger than over the coastal sea, accumulated sensible heat flux should be transported into the coast and results in maximum air temperature just on the coastal inland surface, especially at the point of maximum sensible heat flux convergence. The transportation of accumulated sensible heat flux follows the return flow in the upper level over the coastal sea, which has two atmospheric circulations, such as small circulation in the coastal sea and big one in the open sea.

Compare to surface heating of basin surrounded by only mountains, the transportation of accumulated sensible heat flux from the mountain toward the low atmosphere over the sea can not cause sea waters to be much warmed up, but it can greatly warm up air and soil, since one thousand times higher energy is required to warm up sea water masses than air masses. At this time, air temperature near ground surface of Kangnung city was 35℃, which well matches calculated value, but air temperature on the sea surface is 28℃ less 7℃ than one in the inland coast.

As latent heat flux convergence from the inland coastal surface (250 W/m^2) into the upper level (- 40 W/m^2) is greater than one from the top of the mountain (270 W/m^2) toward the atmosphere (0 W/m^2), some of water vapor evaporated from the coastal inland surface should be transported from the coast into the mountain top and relative humidity is low near the coast and high over the mountain top (Fig. 9b).

4.2.3. Wind field-near sunset

As thermal heating processes of the ground surface and air produced by solar radiation, at 1800 LST around sunset becomes weaken, valley wind and sea breeze also become weaken and thermally induced atmospheric circulation combined with valley-sea breeze becomes shrunken as shown in Fig. 10a and Fig. 10b. Upslope wind combined with valley wind and sea breeze confronts downslope

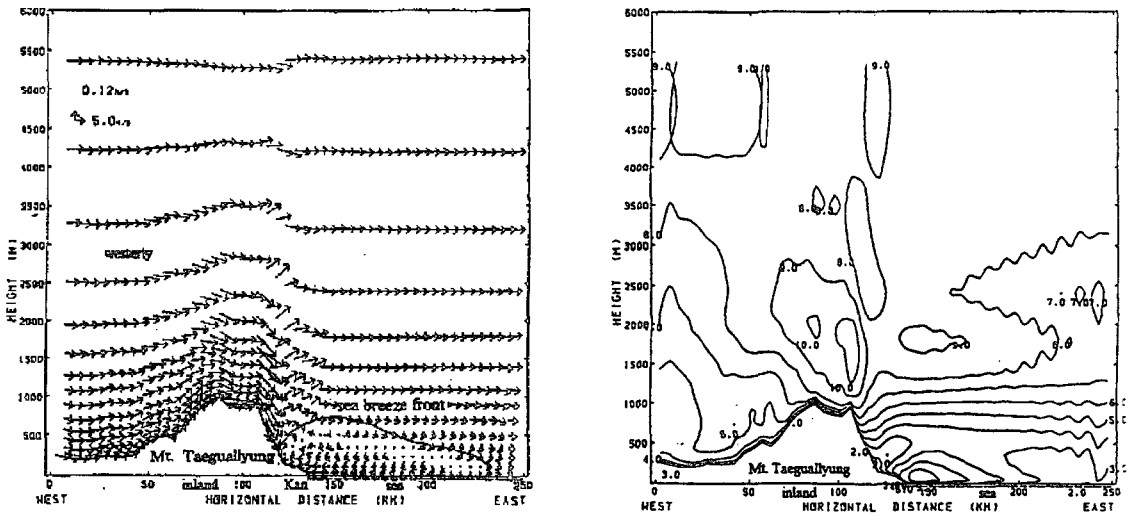

(a) (b)

Fig. 10. (a) Vertical profiles of wind vector (m/s) on a straight cutting line A-B (Mt. Taeguallyung-Kangnung city-East Sea) in a fine-mesh domain at 1800 LST and (b) wind speed (m/s).

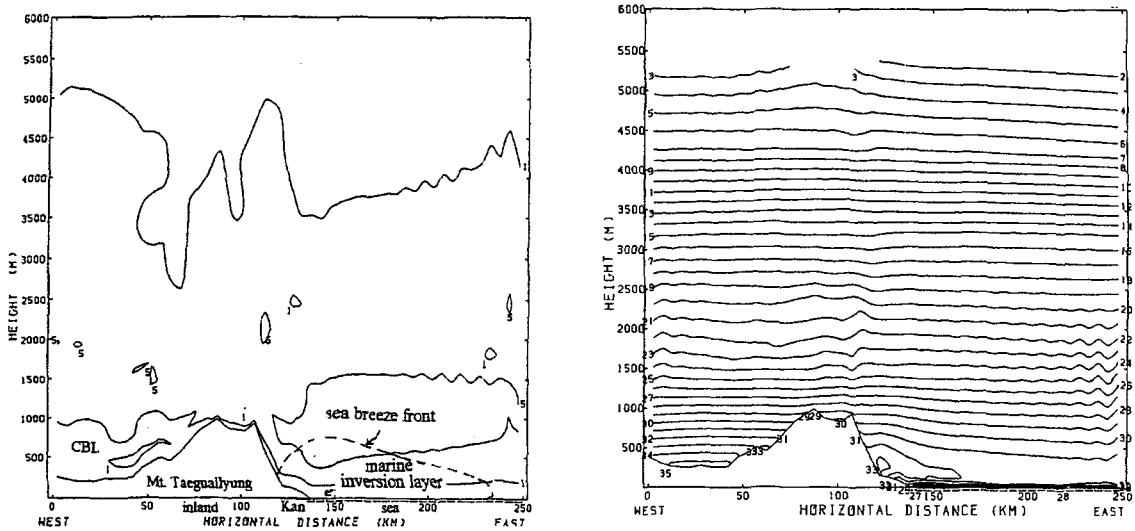

(a) (b)

Fig. 11. (a) As shown in Fig. 10a, except for vertical diffusion coefficient for turbulent heat (m^2/sec) and (b) air temperature (℃).

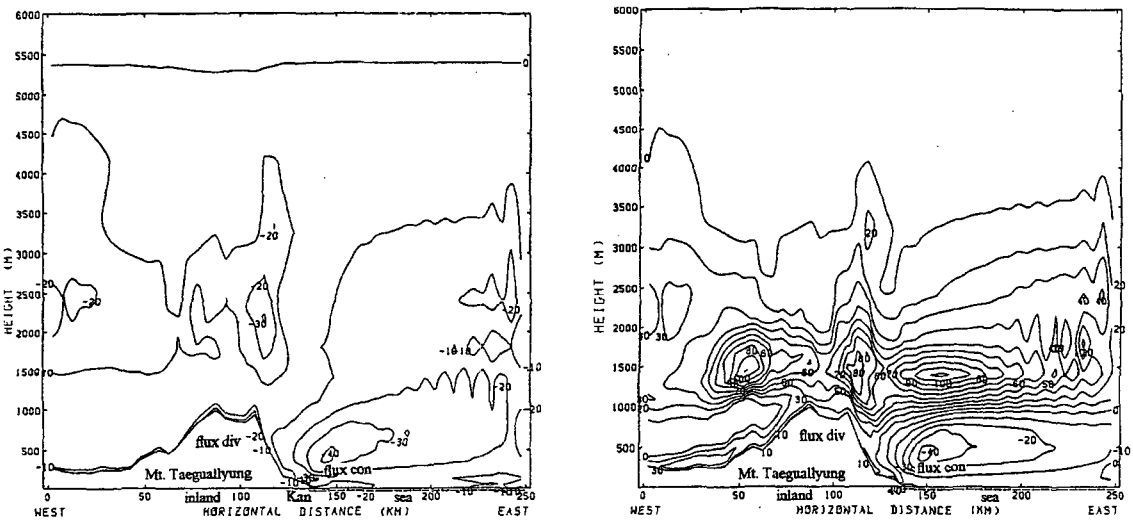

(a) (b)

Fig. 12. (a) As shown in Fig. 10a, except for sensible heat flux (W/m^2) and (b) latent heat flux (W/m^2).

wind blowing over the top of the mountain at about 300 m height along the eastern slope, and then still goes up to the height of 800 m over the ground, becoming a return flow.

Even though the size of atmospheric circulation at 1800 LST is smaller than one at 1200 LST, two circulations with small circulation in the coast and big one in the open sea still exist. Downslope wind speed near the top of the mountain is 7 m/s and one at the confrontation point of the slope is less than 1 m/s. Easterly upslope wind speed near the top of the mountain is 5 m/s and 4 m/s at the coastal edge near Kangnung city, but sea breeze in the coastal sea is 5 m/s. Similarly to 1200 LST, sea breeze starts at the almost same distance of 100 km in the open sea.

4.2.4. Turbulent diffusion and heat flux-near sunset

In Fig. 11a, turbulent diffusion coefficient, K_h is 1 m^2/s over the basin in the west of the mountain and atmospheric boundary is almost neutral, due to very weak thermal heating of the ground surface. This boundary layer is not possible to be called real convective boundary layer with a thickness of hundred meters, because in Fig. 12a, there is no sensible heat flux convergence from the ground surface toward lower atmosphere in the basin. It means the atmospheric boundary layer is in the neutral state. At this time air temperature is 33℃ on the coastal inland surface, showing still high air temperature and 29℃~27℃ on the coastal sea surface (Fig. 11b).

On the other hand, although turbulent diffusion coefficient on the top of the mountain is $1m^2/s$, sensible heat flux divergence from the ground surface of 20 W/m^2 toward lower atmosphere of 10 W/m^2 produces weak nocturnal surface inversion layer less than 100 m. Diffusion coefficient of $1m^2/s$ along the eastern slope to the coast is very small, but sensible heat flux convergence from the surface of 10 W/m^2 toward lower atmosphere of 40 W/m^2 causes thermal heating of air near the surface and produces shallow convective boundary layer or thermal internal boundary layer with a thickness of less than 100 m along the slope and about 200 m in the coast. The diffusion coefficients in the coast and sea are still low with the same magnitude of 1 m^2/s as the daytime one.

Since sensible heat flux convergence along the slope to the coast is greater than over the coastal sea, accumulated sensible heat flux from the coast toward the mountain slope should be transported into the coast, following sea breeze circulation and results in high air temperature of 33℃ at the foot of the mountain and air temperature of 32.5℃ at Kangnung city (Fig. 12a). Air temperature on the coastal sea surface is 27℃ less 1℃ than daytime one (Fig. 11b). Latent heat flux divergence near the top of the mountain cools down air parcel and increases relative humidity, while latent heat flux convergence at the coast still induces evaporation of moisture from the ground surface into the lower atmosphere and relative humidity near the coast is much low than one on the mountain top (Fig. 12b).

4.2.5. Wind field-nighttime

At 0000 LST, August 15, as nighttime radiative cooling of the ground surface due to no solar radiation increases, synoptic south-westerly wind over the top of steep high mountain moves down along the eastern slope toward the coast and is associated with mountain wind generated by air temperature difference

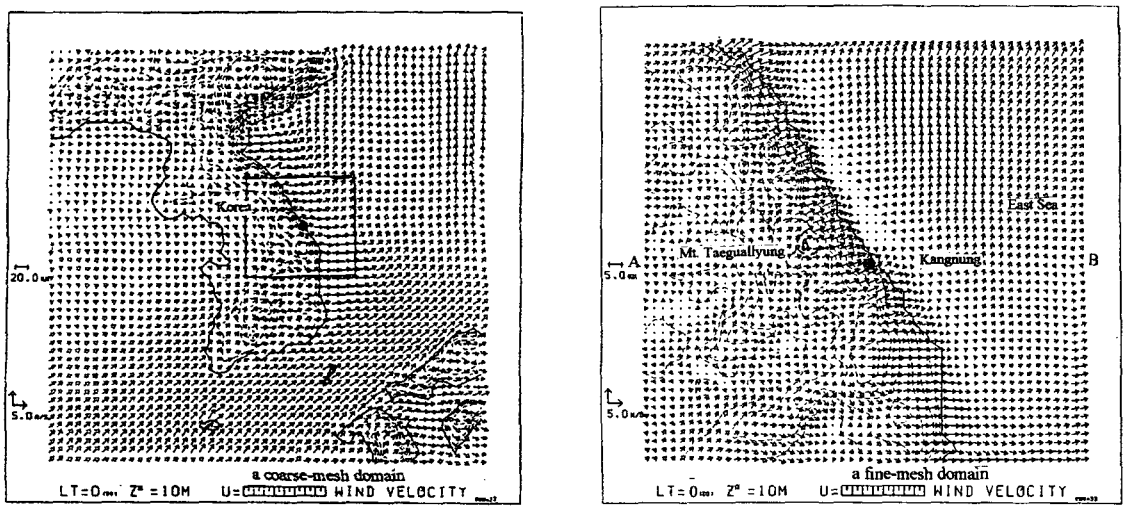

(a) (b)

Fig. 13. (a) Wind vector (m/s) in a coarse-mesh domain at 0000 LST, August 15, 1995. Thin dashline and box denote topography and fine-mesh domain and wind (m/s near Kangnung city) in a fine-mesh domain.

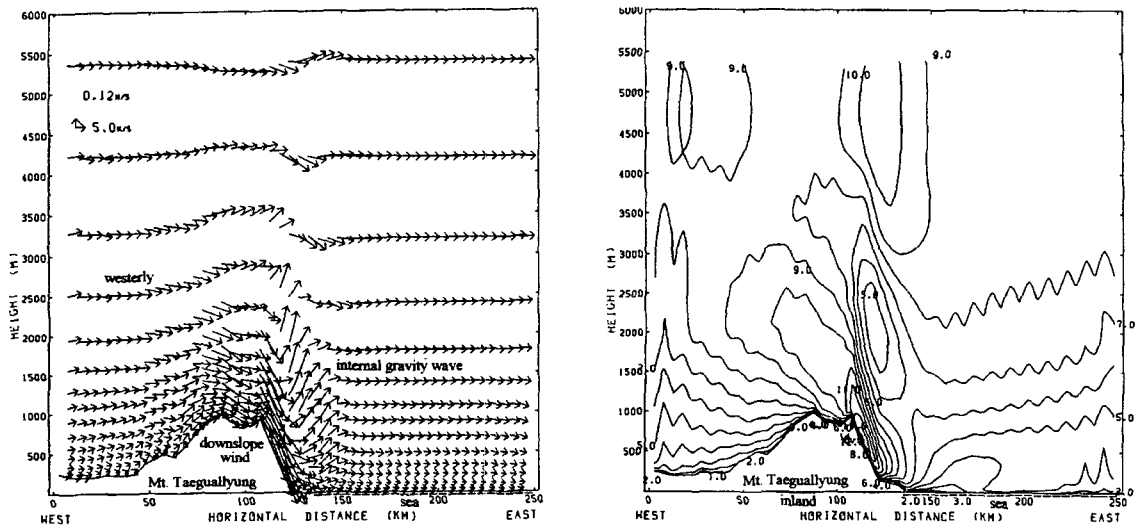

(a) (b)

Fig. 14. (a) Vertical profiles of wind (m/s) on a straight cutting line A-B (Mt. Taegullyung-Kangnung city-East Sea) in a fine-mesh domain as shown in Fig. 13a and (b) wind (m/s).

between the mountain and the plain surfaces, resulting in downslope wind. Then, the downslope wind is further intensified by land breeze due to horizontal air temperature difference between the coastal inland and the sea surfaces, becoming strong downslope windstorm (Fig. 13a and Fig. 13b).

As the downslope windstorm reaching the bottom of the eastern slope is too strong, a hydraulic jump motion of air occurs near the ground surface of Kangnung downtown, bounding up to the 1km height over the coastal sea and causes the generation of lee-side internal gravity waves. Maximum speed of windstorm on the lee slope of the mountain reaches 15 m/s, but nighttime surface wind speed of 2 m/s near Kangnung city beneath of the internal gravity waves is much weaker than daytime one of 5 m/s, under the sea breeze (Fig. 14a and Fig. 14b).

4.2.6. Temperature distribution and heat budget on nocturnal thermal high (tropical night)

Turbulent diffusion coefficients for heat of $1m^2/s$ exists near the ground surface and indicates occurrence of a thin shallow nocturnal surface inversion layer (NSIL). Although its thickness is within the height of about 150 m over the ground in the west of the mountain, no inversion layer due to the destruction of the inversion by strong downslope windstorm is found along the eastern slope and shallow surface inversion layer exists in the coast (Fig. 15a). Falling of potential temperature lines in the lee side of the mountain such as dash line along the slope implies falling of air masses along the eastern slope of the mountain from the upper atmosphere toward the coast and the development of downslope windstorm is expected.

Another dash line in the right hand side indicates the energy propagation of internal gravity waves toward the upper atmosphere (Fig. 15b). Over the sea surface, marine inversion layer (MIL) forms with a thickness of about 250 m. The thickness of the marine inversion layer is slightly larger than one of the inland NSIL, because the cooling of sea surface is much smaller than that of the ground surface. At 0000 LST, surface air temperature at Kangnung city is 29℃, which is over than 25℃ and this temperature continues to be until next day morning. If air temperature over 25℃ persists for whole night, it is called tropical night in the northeastern Asian countries (Fig. 16a).

In Fig. 16b, sensible heat flux of 70 W/m^2 on the surface of the mountain top and that of 10 W/m^2 in lower atmosphere produce sensible heat flux divergence, indicating heat loss at the ground surface and cooling

of ground surface. Sensible heat fluxes of 140 W/m^2 on the eastern slope to 10 W/m^2 in the lower atmosphere also produces a great sensible heat flux divergence along the slope, resulting in great change of air temperature in the narrow atmospheric boundary layer along the slope, as shown in Fig. 16a.

On the other hand, sensible heat fluxes at the inland coastal surface (or coastal sea) and in the lower atmosphere are just 20 W/m^2 (or 10 W/m^2) and 20 W/m^2 (or 10 W/m^2), very small sensible heat flux divergence (or no flux divergence) occurs in the coastal area. So, sensible heat flux divergence is much greater at the mountain top and along the eastern slope than at the coastal inland surface near Kangnung city and the sea surface

It appears that the mountain surface more cools down than the coastal inland surface and the sea surface, and the nighttime air temperatures near the

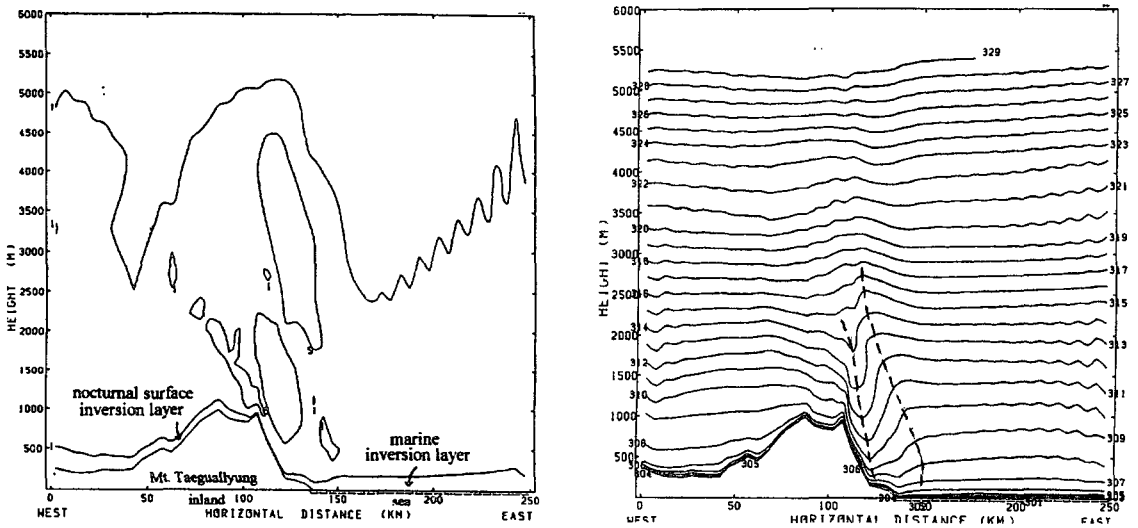

(a) (b)

Fig. 15. (a) As shown in Fig. 14a, except for vertical diffusion coefficient for turbulent heat (m^2/sec) and (b) potential temperature (k).

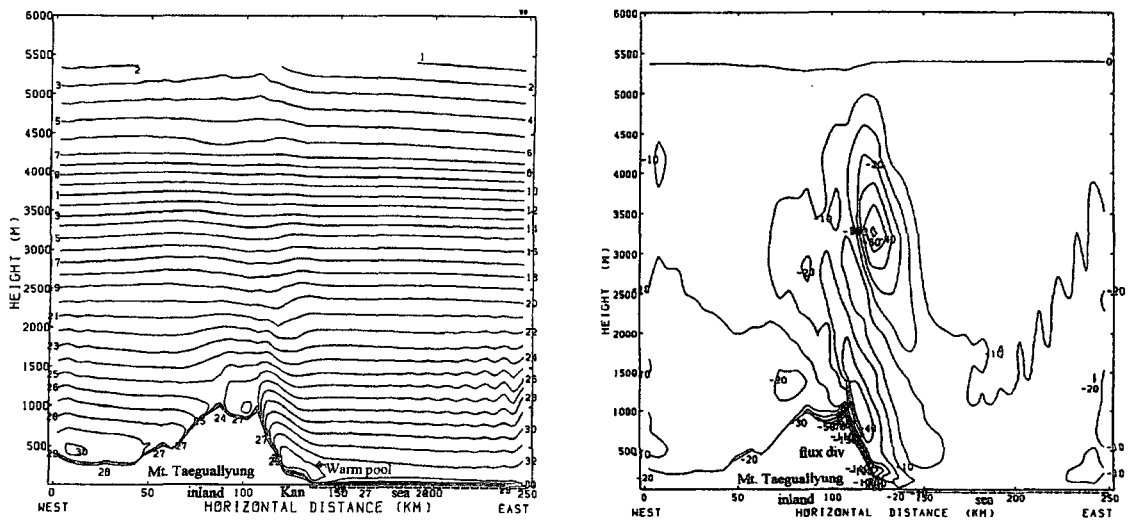

(a) (b)

Fig. 16. (a) As shown in Fig. 14a, except for air temperature (℃) and (b) sensible heat flux (W/m^2).

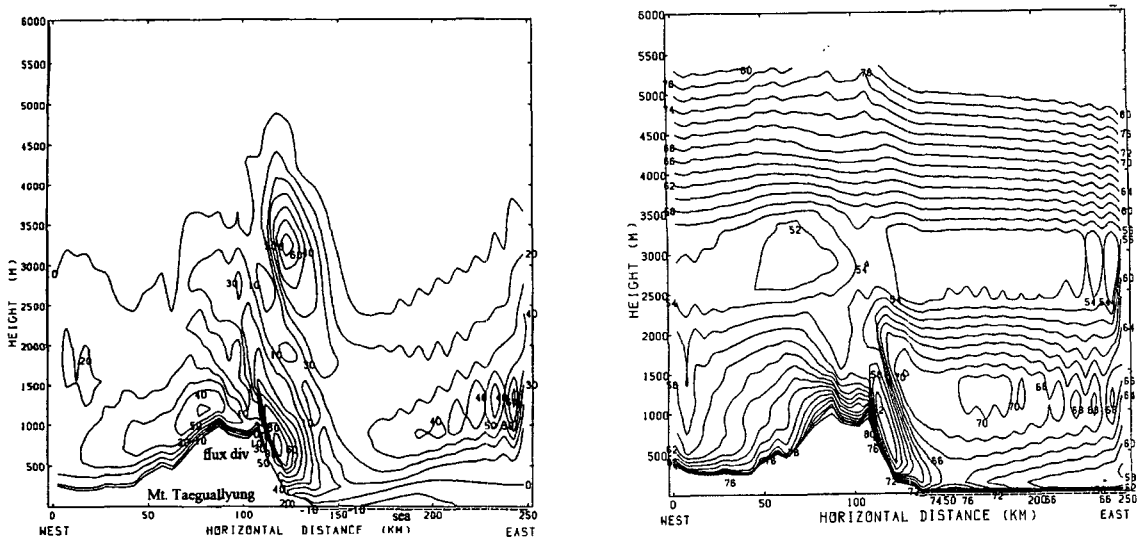

(a) (b)

Fig. 17. (a) As shown in Fig. 14a, except for latent heat flux (W/m^2) and (b) relative humidity (%).

coastal inland and sea surfaces are not much changed from daytime one, resulting in the persistence of nocturnal warming over the coast near Kangnung city and the sea surface and the formation of nocturnal thermal high (tropical night). One of possible mechanism on the formation of tropical night is some amount of heat transfer from warm pool of 34℃ into the coastal surface, penetrating through very shallow nocturnal surface inversion layer less than 100m depth and then, the transfer of the long wave radiation toward the surface could prevent from the rapid cooling of the coastal surface.

As latent heat fluxes on the surfaces of the mountain top and along the eastern slope are 10 W/m^2 and 50 W/m^2, but they are 50 W/m^2 and 90 W/m^2 in the lower atmosphere, latent heat flux divergence occurs on the mountain top and along the eastern slope. The rapid cooling of the ground surface increases moisture content on the mountain surface (Fig. 17a). It induces high relative humidity of 80 % on the surface of the mountain top and 72 % along the slope surface. On the other hand, in the area away from the eastern slope of the mountain, minimum relative humidity is 52 %.

Latent heat fluxes near the inland coastal surface toward the lower atmosphere are 10 W/m^2 to 10W/m^2 and the fluxes from the coastal sea surface toward the lower atmosphere are -10 W/m^2 to 20 W/m^2, with a relatively smaller difference than one in the mountainside, respectively. Thus, it induces high relative humidity of 72 % and 74% in the coast and coastal sea surface (Fig. 17b).

Outside of shallow boundary lay along the slope, that is, at the level of 1km height in the propagation route of international gravity waves (Fig. 15b), relative humidity increase to 70 %. The increase of relative humidity is mainly due to the supply of some amount of moisture from the sea surface under the uplifted wind and the cooling of the moist air.

4.2.7. Wind field-early morning

Wind fields in Korean peninsula and Kangnung coastal area at 0600 LST, August 15 are similar to the ones at 0000 LST. As the time of 0600 LST is just after sunrise, the sea and land surfaces are not sufficiently heated by solar radiation, resulting in persistent existence of cool air masses over the land and sea surfaces and no formation of easterly sea breeze in the visual display. Thus, under westerly and south-westerly synoptic wind, westerly offshore wind combined with downslope wind and land breeze still prevails in the Kangnung coastal region. This is a reason why calm zone in Fig 18a, due to the conflict of westerly offshore wind with easterly onshore wind (basically weak sea breeze) is more widely extended in the coastal sea, comparing to the calm zone at 0000 LST (Fig. 3b, Fig. 18b).

On the vertical profile of wind in Fig. 19a and 19b, there is still strong downslope wind along the eastern slope the mountain and bounds up toward the low atmosphere, with a hydraulic jumping motion, reaching to the about 3.5 km height above the ground surface of the inland coastal region. The area of maximum wind speed of 14 m/s is located closing to the top of the mountain. It means that even though there is no visualization of weak easterly onshore wind combined with valley wind and sea breeze starts from the coastal sea toward the mountain, it faces westerly offshore wind combined with mountain wind and land breeze, resulting in the slightly uplifted area of maximum wind speed toward its top.

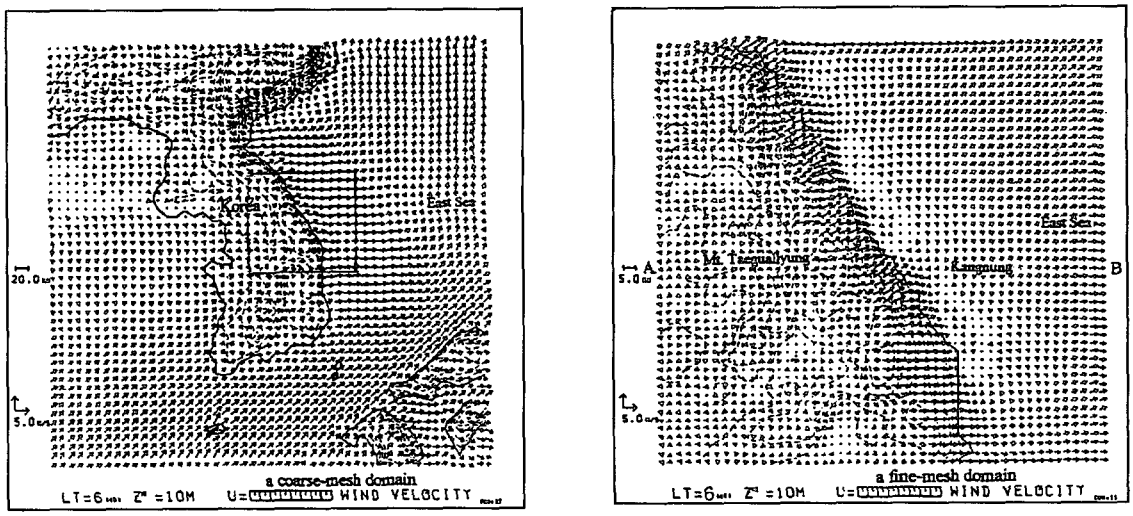

(a) (b)

Fig. 18. (a) Wind vector (m/s) in a coarse-mesh domain at 0600 LST, August 15, 1995. Thin dashline and box denote topography and fine-mesh domain and wind (m/s near Kangnung city) in a fine-mesh domain.

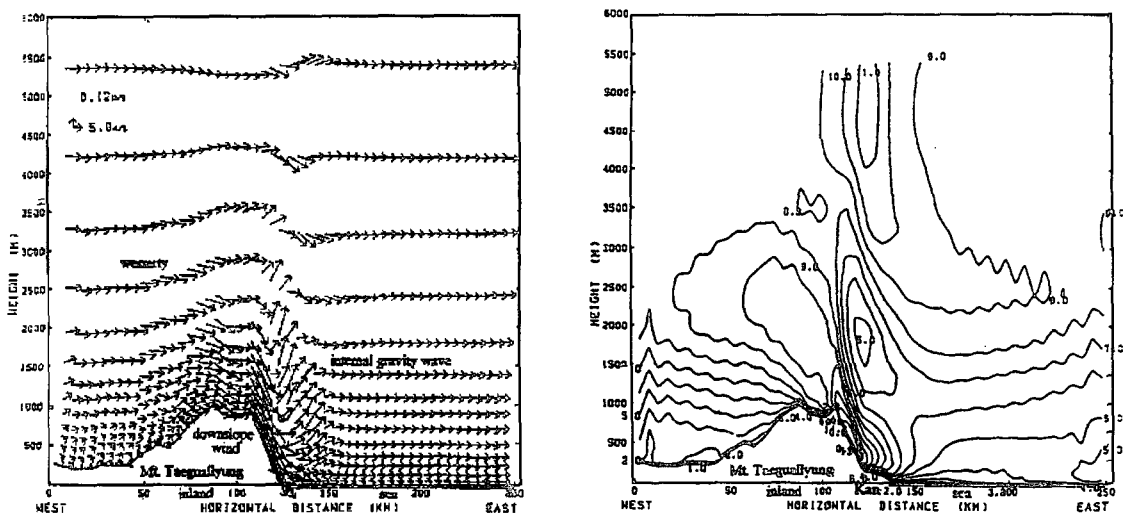

(a) (b)

Fig. 19. (a) Vertical profiles of wind (m/s) on a straight cutting line A-B (Mt. Taeguallyung-Kangnung city-East Sea) in a fine-mesh domain at 0600 LST, August 15, 1995 and (b) wind (m/s).

4.2.8. Turbulent diffusion and heat fux-early morning

A thin shallow nocturnal surface inversion layer with turbulent diffusion coefficients for heat of 1 m^2/s exists near the ground surface and its thickness is about 150 m over the ground in the west of the mountain, but no inversion layer exists due to the destruction of the inversion by strong wind over 8 m/s in the top of the mountain and strong downslope wind over than 10 m/s along the eastern slope of the mountain (Fig. 20a). Over the sea surface, marine inversion layer of 20℃ near the sea surface to 31℃ in the higher level still forms with a thickness of about 200 m (Fig. 20b). The thickness of the marine inversion layer is slightly larger than one of the inland NSIL, because the cooling of sea surface is

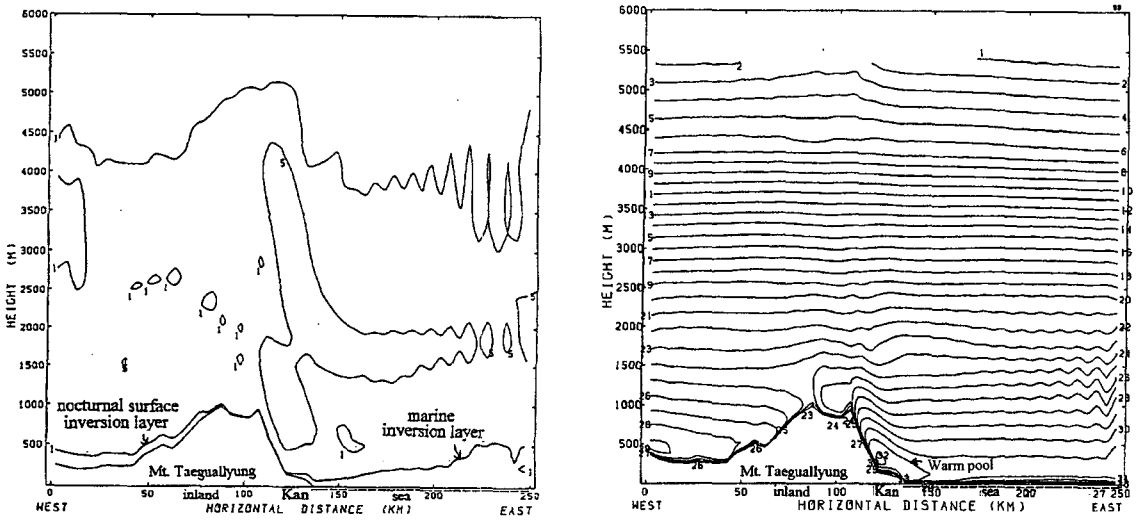

(a) (b)

Fig. 20. (a) As shown in Fig. 18a, except for vertical diffusion coefficient for turbulent heat (m^2/sec) and (b) air temperature (℃).

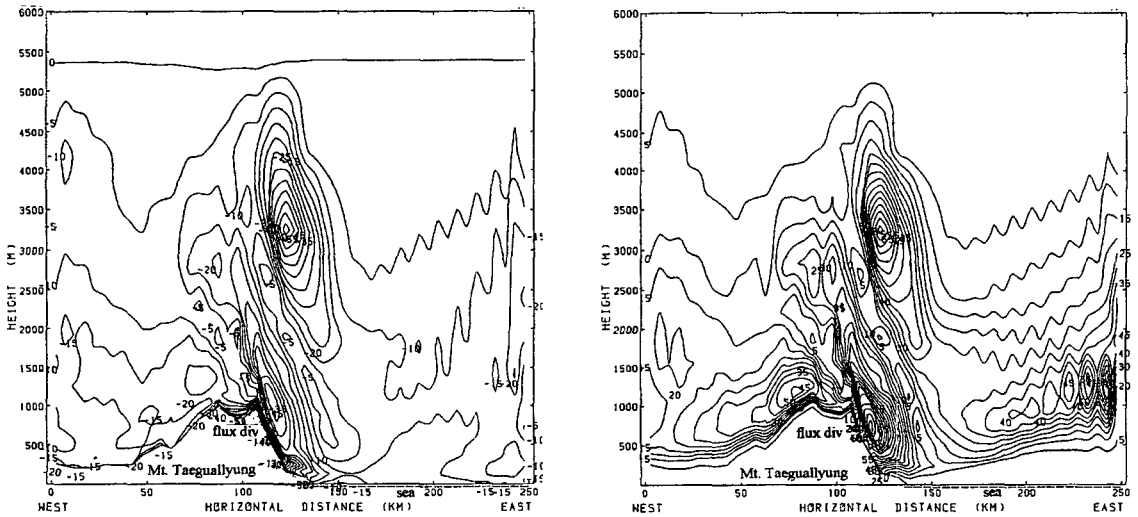

(a) (b)

Fig. 21. (a) As shown in Fig. 18a, except for sensible heat flux (W/m^2) and (b) latent heat flux (W/m^2).

much smaller than that of the ground surface.

As warm pool of 32℃ at 0600 LST is still located in the lower atmosphere over the coastal inland (Kangnung city) and coastal sea and long wave radiation fluxes from the warm pool are toward both atmosphere and surfaces. Even though the cooling of ground surface under no solar radiation reduces the decrease of air temperature near the surface, the long wave radiation toward the surface can compensate the reduction of cooling rate of the ground surface, resulting in still existence of a high air temperature near the surface like nocturnal thermal high. The surface air temperature at Kangnung city is 26.5℃ over than 25℃, which is the temperature condition of the existence of tropical night, and it continues to be from 0000 LST to 0600 LST. The different sensible heat flux divergence between mountain and coast is mainly due to the different heat capacities of soil, air and sea.

Since sensible heat flux from the surface of the mountain top toward the lower atmosphere is with 50 W/m^2 to 10 W/m^2 and the flux from the foot of the mountain toward the atmosphere is 140 W/m^2 to 10 W/m^2, the vertical distribution of sensible heat fluxes produces sensible heat flux divergence, which indicates heat loss at the ground surface and cooling of ground surface, similar to those at 0000 LST (Fig. 16b and Fig. 21a). Sensible heat fluxes of 140 W/m^2 on the eastern slope to 10 W/m^2 in the lower atmosphere also produces a great sensible heat flux divergence along the slope, resulting in great change of air temperature in the narrow atmospheric boundary layer along the slope to the bottom of the mountain (that is, thermal internal boundary layer).

On the other hand, sensible heat fluxes at the inland coastal surface of Kangnung city (Kan) (and coastal sea) and in the lower atmosphere are just 20 W/m^2 (or 10 W/m^2) and 10 W/m^2 (or 10 W/m^2). This distribution produces a very small sensible heat flux divergence (or no flux divergence) in the coastal area. So, sensible heat flux divergence is much greater at the top of the mountain and along the eastern slope than at the coastal inland surface near Kangnung city and the sea surface. It appears that the mountain surface more cools down than the coastal inland surface and the sea surface, and the nighttime air temperatures near the coastal inland and sea surfaces are not much changed from daytime one, resulting in the persistence of nocturnal warming over the coastal basin (Kangnung city) and the sea surface and the formation of nocturnal thermal high (tropical night).

As latent heat fluxes from the surfaces of the mountain top and the eastern slope of the mountain toward the lower atmosphere are 5 W/m^2 to 45 W/m^2, and 50 W/m^2 to 90 W/m^2, latent heat flux divergence is similar to the flux distribution at 0000 LST occurs on the top of the mountain and along the slope. Under this circumstance, moisture contents of air masses on the mountain surface may be still high, due to the great cooling of air masses near the surface and relative humidity near the mountain surface should be almost the same as one at 0000 LST (Fig. 21b).

On the other hand, latent heat flux near the coastal basin surface and the coastal sea surface toward the lower atmosphere has 5 W/m^2 to 25 W/m^2 and 5 W/m^2 to 5 W/m^2 with a relatively small difference or no difference of latent heat flux. Thus, it induces same moist content high relative humidity of 72 % along the slope and low relative humidity of 64 % at the coast.

4.2.9. Wind field next day daytime

At 0900 LST, August 15, two different wind regimes still confront each other in the bottom of the mountain at the distance of 10 km away from the coast. As shown in Fig. 22a and 22b, after sea breeze starts at 50km offshore and combines with valley wind in the coastal plain near Kangnung city toward the mountain, it becomes an intensified onshore wind and reaches to the foot of the mountain. Simultaneously, prevailing synoptic scale westerly wind blows over Mt. Taeguallyung toward the coast and it confronts the onshore wind along its eastern slope and then, it goes up toward the level of 500 m and becomes a return flow over the sea (Fig. 22a and 22b).

4.2.10. Temperature distribution and heat budget-next day daytime

In Fig. 23a, the value of vertical diffusion coefficients for turbulent heat, K_h is more than $60m^2/s$ over the plain in the west of the mountain and the top. On the other hand, the vertical turbulent coefficient along the eastern slope of the mountain and over the coastal inland basin and sea surface are 5 m^2/s and 1 m^2/s. Higher values of the diffusion coefficients found in the west of the mountain and the top than

along the slope and over the coast is due to greater diabatic (or non-adiabatic) heating on the mountain surface. The area with high turbulent heat diffusivity (or vertical diffusion coefficients for turbulent heat) indicates convective boundary layer and its depth is about 200 m in the west of the mountain.

A shallow boundary layer along the eastern slope is also found with a thickness of about 100 m, but it is not strong due to weak turbulent diffusivity. As shown in Fig. 23b, in the foot of the mountain and inland coastal basin, a shallow thermal internal boundary layer with a maximum air temperature of 34℃ near

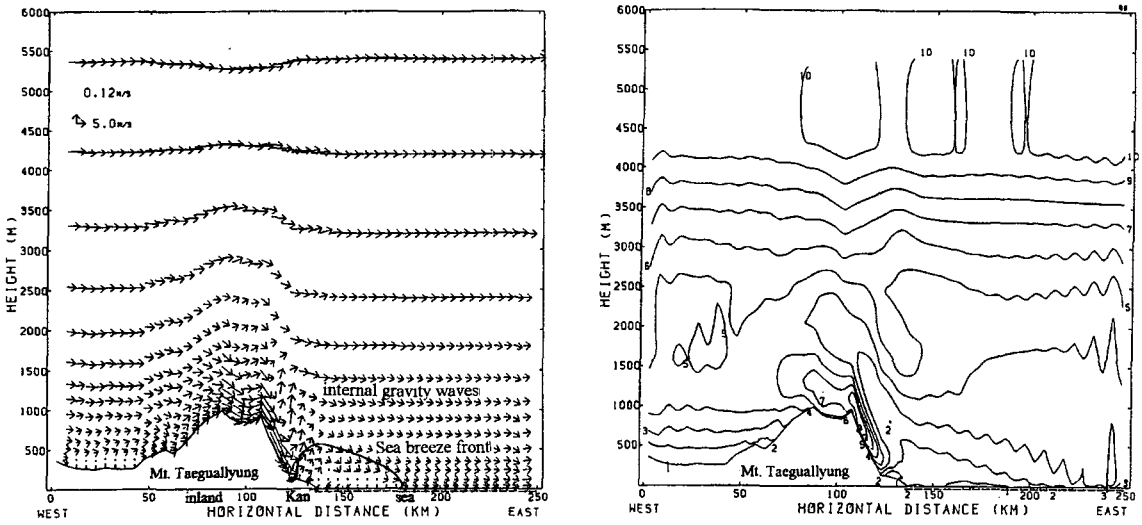

Fig. 22. (a) Vertical profiles of wind (m/s) on a straight cutting line A-B (Mt. Taegullyung-Kangnung city-East Sea) in a fine-mesh domain at 0900 LST, August 15, 1995 and (b) wind (m/s). Three different kinds of wind regimes such as westerly downslope wind, internal gravity and sea-breeze.

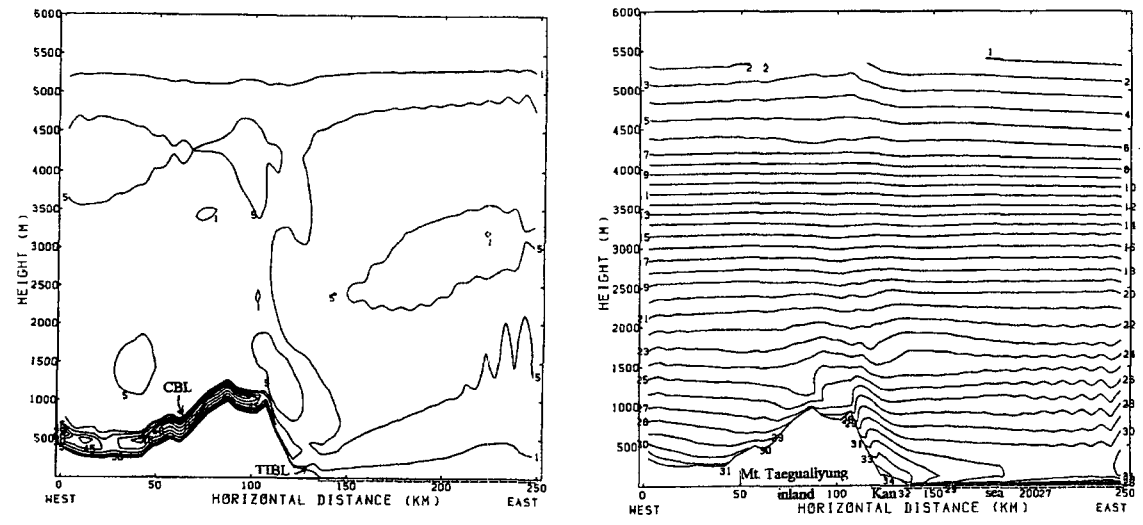

Fig. 23. (a) As shown in Fig. 22a, except for vertical diffusion coefficient for turbulent heat (m^2/sec) and (b) air temperature (℃).

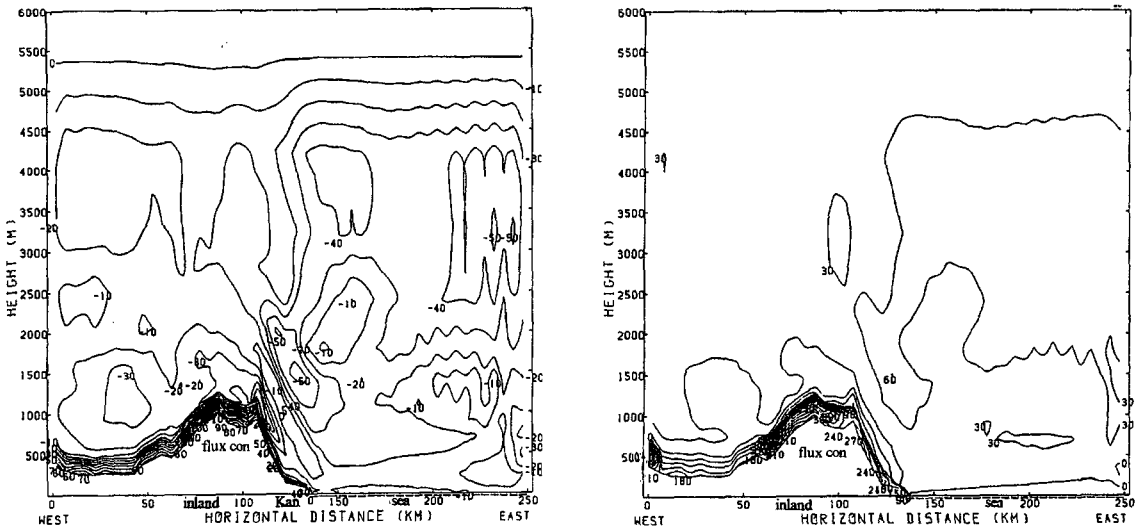

Fig. 24. (a) As shown in Fig. 22a, except for sensible heat flux (W/m^2) and (b) latent heat flux (W/m^2).

the surface is developed, while marine atmospheric inversion layer still exist, due to air temperature of 33℃~31℃ higher than the air temperature of 29℃ ~27℃ on the sea surface. In Fig. 24a, sensible heat fluxes from the surface of the top of mountain toward the upper level are in a range of 90 W/m^2 to -20 W/m^2 within about 300 m and those from the eastern slope of the mountain toward the upper level are also from 50 W/m^2 to 10 W/m^2 within 200 m, showing sensible heat flux convergence. This sensible heat flux convergence indicates the thermal heating of air masses from the ground surface and the increase of air temperature. Thus there must be the development of convective boundary layer.

Sensible heat fluxes from the coastal basin surface toward the upper atmosphere are 40 W/m^2 to 10 W/m^2 within 100 m and it shows the sensible heat flux convergence, resulting in the development of shallow thermal internal boundary layer in the inland coast and the increase of air temperature to 34℃. The accumulated sensible heat flux under the influence of sea breeze circulation returning down to the coast should be transported into the coast, resulting in the increase of air temperatures near the coastal inland.

On the other hand, the fluxes from the coastal sea and open sea surfaces toward the upper levels are from 20 W/m^2 to 20 W/m^2 and from one less than 10 W/m^2 to 10 W/m^2, respectively. No sensible heat flux divergence causes no cooling of air, while the flux divergence drives the cooling of air near the open sea surface, resulting in the formation of inversion layer

Similar tendency to the sensible heat flux, latent heat fluxes from the surface of the top of mountain toward the upper level are 240 W/m^2 to 30 $W/m^2$and those from the eastern slope of the mountain including the coastal basin toward the upper level are from 270 W/m^2~240 W/m^2 to 30 W/m^2, showing latent heat flux convergence (Fig. 24b). This distribution drives evaporation of water particles from air mass, enhancing the drought of moist content of air and the rapid increase of air temperature under low moist

Table 1. Comparison of calculated air temperature (℃) to observed one at Kangnung city from August 14 through 15, 1995

Date	Comparison	1200	1500	1800	2100	0000	0300	0600	0900
8/14~8/15	Observed	35.0	34.6	33.4	30.0	29.8	27.6	26.5	29.9
	Calculated	35.0	34.0	32.5	30.0	29.0	29.0	29.0	32.0

content of air.

However, the latent heat fluxes from the coastal sea toward the upper levels, which are from 90 W/m^2 to 30 W/m^2 indicate latent heat flux convergence and causes evaporation of water particles from air. The heat fluxes from open sea surfaces toward the upper levels, which are from 0 W/m^2 to 0 W/m^2 drive no sensible heat flux divergence and causes no evaporation and condensation process of air., keeping almost constant moist content of air to the one at the previous time.

4.2.11. Comparison of observed air temperature with calculated one by a model

In order to investigate the occurrence of tropical night over than 25℃ of air temperature at Kangnung coastal city, calculated air temperatures were compared with the observed ones during the period of tropical night from August 14 through 15, 1995[19]. General tendency of calculated values well matched the observed ones with a discrepancy of about 6 % for whole period, but the discrepancy for the nighttime, especially for the occurrence of tropical night was less than 5 %. Thus, considering the atmospheric boundary layer process of wind fields, turbulent heat, sensible heat flux, latent heat flux, air temperature can be evaluated and tropical night can also be spatially and temporally predicted.

5. Conclusions

Although hot night called tropical night in summer of northeastern Asia has often occurred, no one has explained the driving mechanism on the formation of tropical night so far. This study was focused on the investigation of driving mechanism for the formation of tropical night in the coastal region from August 14 through 15, 1995.

Convective boundary layer with a 1km depth is developed over the ground surface of the inland basin in the west of the mountain and near the top of the mountain, while a depth of thermal internal boundary layer less than 150m from the coast along the eastern slope of the mountain.

As sensible heat flux convergences from the surface of the mountain top and the inland coastal surface toward lower atmosphere are much greater than that on the coastal sea, sensible heat fluxes should be accumulated inside both the thermal internal boundary layer and the convective boundary layer near the mountain top. Then, accumulated sensible heat flux under the influence of sea breeze circulation returning down to the coast should be transported into the coast, resulting in high air temperatures near the coastal inland.

At night, mountain wind causes the daytime existed westerly wind to be an intensified westerly downslope wind under no upward valley wind and land breeze further induces it to be strong wind. No sensible heat flux divergence or very small flux divergence occurs in the coast, while the flux divergences are much greater at the top of the mountain and along its eastern slope than on the coastal inland and sea surfaces. Less cooling down of the coastal surface than the mountain surface and sensible heat transfer from warm pool of 34^0 into the coastal surface make nocturnal air temperature on the coastal inland surfaces to be not much changed from daytime ones, resulting in the persistence of nocturnal thermal high (tropical night) until the early in the morning

Acknowledgements

Author thanks Mr. Takahashi, Japan Meteorological Agency for helpful comment on this research and further thanks to Dr. S. Sato, Japan Meteorological Research Institute for using Hitachi super computer.

References

1) Raynor, G. S., S. SethuRaman and R. M. Brown, 1979, Formation and characteristics of coastal internal boundary layer during onshore flows, Boundary Layer Meteor., 16, 4587-514.
2) Pielke, R. A., 1984, Mesoscale meteorological modeling, Academic Press, 612pp.
3) Kondo, J, T. Kuwagata and S. Haginoya, 1989, Heat budget analysis of nocturnal cooling and daytime heating in a basin, J. Atmos. Sci., 46, 2917-2933.
4) Whiteman, C. D., 1990, Observations of thermally developed wind system in mountainous terrain, Atmospheric Processes over complex terrain, Meteor. Monogr., Amer. Meteor. Soc., 40, 5-42.
5) Kuwagata, T., M. Sumioka, N. Masuko and J. Kondo, 1990, The daytime PBL heating process

over complex terrain in central Japan and fair and calm wether conditions, Part 1: Meso-scale circulation and the PBL heating rate, J. Meteor. Soc, Japan, 68, 625-638.

6) Choi, H. and J. Kim, 1997, Three-dimensional numerical prediction on the evolution of nocturnal thermal high (tropical night) in a basin, Korean J. Geophy. Res., 25(1), 57-81.
7) Choi, H., 2003, Increase of ozone concentration in an inland basin during the period of nocturnal thermal high, Water, Air & Soil Poll: Focuss, 3, 31-52.
8) Choi, H., 2004, Persistent high concentration of ozone during windstorm conditions in southern Korea, Meteor. & Atmos. Phys., 87, 93-107.
9) Choi, H., Y. H. Zhang and S. Takahashi, 2004, Recycling of suspended particulates by the interaction of sea-land breeze circulation and complex coastal terrain, Meteor. & Atmos. Phys., 87, 109-120.
10) Takahashi, S., 1997, Manual of LAS model revised by Dr. J. Sato, Meteorological Research Institute of Japan, 50pp.
11) Klemp, J. B. and D. R. Durran, 1983, An upper condition permitting internal gravity wave radiation in numerical mesoscale models, Mon. Wea. Rev., 111, 430-440.
12) Orlanski, I., 1976, A simple boundary condition for unbounded hyperbolic flows, J. Comp. Phys., 21, 251-269.
13) Yamada, T., 1983, Simulation of nocturnal drainage flows by a q2-l turbulence closure model, J. Atmos. Sci., 40, 91-106.
14) Yamada, T. and G. L. Mellor, 1983, A numerical simulation of the BOMEX data using a turbulence closure model coupled with ensemble cloud relations, Q. J. R. Meteor. Soc., 105, 95-944.
15) Katayama, A. 1972, A simplified scheme for computing radiative transfer in the troposphere, Technical report No. 6, Dept. of Meteor., U.C. L.A., 77pp.
16) Businger, J. A., 1973, Turbulence transfer in the atmospheric surface layer, In Workshop on micrometeorology (D. A. Haugen, ed), Amer. Meteor. Soc., 67-100pp.
17) Monin, A. S., 1970, The atmospheric boundary layer., Annual Review of Fluid Mechanics, 2, 225-250.
18) Deardoff, J. W., 1978, Efficient prediction of ground surface temperature and moisture with inclusion of a layer of vegetation, Geophys. Res., 38, 659-661.
19) KMA, 1995, Observed data made by Kangnung Meteorological Administration.